Thermochimica Acta 486 (2009) 20–26

Contents lists available at ScienceDirect

Thermochimica Acta

journal homepage: www.elsevier.com/locate/tca

Reduction/reoxidation of a multicomponent molybdate catalyst for propylene ammoxidation

Xinying Wu[a], Guangren Yu[a], Xiaochun Chen[a,*], Yahui Wang[b], Changjiang Liu[a]

[a] College of Chemical Engineering, Beijing University of Chemical Technology, Beijing 100029, China
[b] Petrochemical Process Department, Sinopec Engineering Incorporation, Beijing 100101, China

ARTICLE INFO

Article history:
Received 9 July 2008
Received in revised form 9 November 2008
Accepted 15 December 2008
Available online 24 December 2008

Keywords:
Reduction
Reoxidation
Crystal structure
Thermogravimetric analysis
Multicomponent molybdate catalyst

ABSTRACT

The reduction/reoxidation mechanism of a multicomponent molybdate catalyst for propylene ammoxidation was studied by using X-ray powder diffraction (XRD), Laser Raman spectroscopy (LRS) and thermogravimetric analysis methods. XRD and LRS results of the catalysts with various reduced degrees show that catalyst reduction happens in the order: (2)→(3)→(4)→(5), and the lattice oxygen migration range is extended from iron molybdates to cobalt/nickel molybdate. The thermogravimetric analysis results show that the reoxidation of the catalyst is attributed to the replenishment of the bulk lattice oxygen in the lower temperature which is respectively combined with Bi, Fe and Mo, and the replenishment of the surface lattice oxygen in the higher temperature. The favorable reoxidation temperature is found to be around 440 °C.

1. Introduction

Acrylonitrile (AN) is a versatile intermediate for chemical synthesis, and propylene ammoxidation is widely used to produce AN in industry [1,2]:

$$CH_2=CHCH_3 + NH_3 + \frac{3}{2}O_2(air) \xrightarrow{catalyst} CH_2=CHCN + 3H_2O \quad (1)$$

Turbulent fluidized bed (TFB) technique is widely adopted, with the advantages of effective heat/mass transfer and easy temperature control. Propylene ammoxidation obeys a redox mechanism [3–5], i.e., the lattice oxygen in catalyst reacts with propylene/ammonia to generate AN, and the reduced catalyst is continuously reoxidized in situ by gaseous oxygen in TFB reactor. However, due to severe axial gas/solid backmixing and insufficient gas/solids contact in such TFBs, AN generally suffers from an overoxidation and some byproducts such as CO_2 are produced [6], which was also found by our modeling studies [7,8]. Obviously, propylene ammoxidation in such TFBs is against the green chemistry concept of high selectivity and low yields of byproducts such as CO_2 [9].

With regard this, circulating fluidized bed (CFB) has been attempted to perform propylene ammoxidation [6,10–16], where lattice oxygen, propylene and ammonia react in a riser with excluding gaseous oxygen, and catalyst reoxidation is performed in another separate regenerator. In fact CFB is used now for the production of maleic anhydride and ethylene which obey redox mechanism [17–19]. There are many advantages in such CFBs, (a) AN overoxidation and CO_2 yield are substantially suppressed because of no or little amount of gaseous oxygen in riser; (b) due to no trouble with explosion limit, a highly concentrated propylene/ammonia feed can be used, i.e., higher throughput; (c) the succeeding separation processes are simplified from a less production of byproducts.

In such CFB processes, the study on the separate reduction and reoxidation of catalysts is important for optimizing the catalyst design or the CFB process. Bismuth molybdates are the most popular catalysts and have been the emphasis of wide studies. Some studies were focused on the co-feed of propylene/ammonia/air(oxygen) in TFB [20–22], where the oxidation state of catalyst keeps almost no change because of the reoxidation in situ of catalyst by gaseous oxygen. Anion vacancy and lattice oxygen diffusion were investigated in different bismuth molybdate catalysts including $Bi_2(MoO_4)_3$, $Bi_2Mo_2O_9$, and Bi_2MoO_6 [23,24], where H_2 as reductant. The reduction of $Bi_2(MoO_4)_3$ by propylene/ammonia in absence of gaseous oxygen showed that $Bi_2(MoO_4)_3$ is first transformed into Bi_2MoO_6, and the latter finally is reduced into MoO_2 and Bi [25]. The reoxidation study of partial reduced $Bi_2(MoO_4)_3$, $Bi_2Mo_2O_9$, Bi_2MoO_6, $Bi_3FeMo_2O_{12}$, and $M_a^{2+}M_b^{3+}Bi_xMo_yO_z$ showed that there exist two reoxidation regimes, i.e., the separate reoxidation of surface and bulk lattice oxygen [26]. The multicomponent molybdate catalysts are continuously developed. Some studies on reduction of it in absence of gaseous oxygen were carried out, in order to investigate the effect of

* Corresponding author. Tel.: +86 10 64421370; fax: +86 10 64421370.
E-mail address: buctchenxc@126.com (X. Chen).

0040-6031/$ – see front matter © 2009 Elsevier B.V. All rights reserved.
doi:10.1016/j.tca.2008.12.018

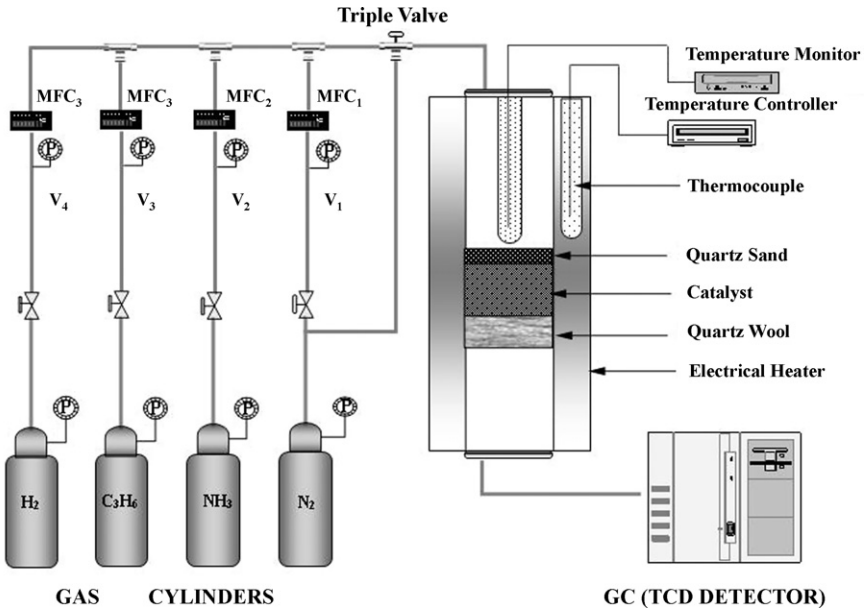

Fig. 1. Experimental schematic of catalyst reduction, MFC_1–MFC_4: mass flow controller, V_1–V_4: constant pressure valve.

lattice oxygen mobility on its activity and selectivity [27], its reactivity of surface oxygen species [28], and its reduction kinetics [26,29]. Some studies on reoxidation of the partial reduced catalyst were carried out, in order to investigate its regeneration performance [30] and its reoxidation kinetics [26]. Some studies on the kinetics of reduction/reoxidation were investigated under co-feed situation, showing that the main reaction was controlled by the reduction step of the catalyst at high temperature and by the reoxidation step at low temperature [31,32].

The aim of the present work is to study the separate reduction/reoxidation of a selected multicomponent molybdate catalyst ($M_a^{2+}/M_b^{3+}Bi_xMo_yO_z$) by using XRD, LRS and thermogravimetric analysis methods (including thermogravimetry, TG and differential thermogravimetry, DTG). The crystal and surface structures of fresh, reduced and reoxidized catalysts, and the TG/DTG curves for the reoxidation catalysts are given; following these characterization, the reduction/reoxidation mechanism is discussed.

2. Experimental

The catalyst is from Shanghai Research Institute of Petrochemical Technology (SRIPT), China. In order to ensure the full oxidation of catalysts, they are calcined first in air at 450 °C for 4 h. Ammonia, hydrogen, nitrogen and oxygen used in the reaction are 99.999% (made in Beijing ZG Gases Science & Technology Co., Ltd.), and propylene is 99.99% (made in Sinopec Qilu Co., Ltd.).

2.1. Reduction

The experimental schematic is shown in Fig. 1. The experiments are carried out in a fixed bed reactor, which is a stainless steel tube of 8 mm i.d. and 200 mm of height. The reaction section is packed with around 0.7 g catalyst, above which is quartz sand and below is quartz wool. The reaction temperature is about 450 °C, which is controlled by electrical heater; the operation pressure is atmospheric. During the reduction process, a mixed gaseous feed of propylene, ammonia and nitrogen with a molar ratio of 1:1.3:9, or hydrogen and nitrogen with a molar ratio of 1:4, is introduced into the reactor with a flow rate of 62 ml/min, which is controlled by mass flow controller. The reduced time by propylene/ammonia includes 15 s (catalyst A), 30 s (catalyst B), 45 s (catalyst C), and 60 s (catalyst D). The reduced time by hydrogen includes 10 s (catalyst E), 25 s (catalyst F), 40 s (catalyst G), and 55 s (catalyst H). The reaction products were analyzed online by East & West 4000A gas chromatograph with a thermal conductivity detector, when the reduced time by propylene/ammonia is 15, 30, 45 and 60 s, respectively. The H_2 flow through the columns consisting of molecular sieve 5A and Porapak Q was held constant 25 ml/min.

2.2. Reoxidation

The reoxidation of the reduced catalyst is monitored by Netzsch STA 449C thermo-analyzer. The oxidation gases consist of oxygen and argon with a molar ratio of 1:1, and the flow rate is 60 ml/min. The catalyst loading is around 20 mg. The temperature increasing rate is 5 °C/min.

2.3. Characterization

XRD is performed on Rigaku D/Max2500 VB2 + PC with Cu Kα radiation at room temperature. Scans are performed over the 2θ range from 15° to 65° recorded with a position sensitive detector.

LRS is performed on a Jobin Yvon HR800 confocal spectrometer equipped with a semiconductor laser supplying the excitation line at 532 nm with a power of 2 mW. Measurements were carried out with a resolution of 0.5 cm^{-1}.

3. Results and discussion

3.1. Reduction

3.1.1. Reduction by propylene/ammonia in absence of gaseous oxygen

The XRD patterns for the fresh and reduced catalysts are shown in Fig. 2, and the crystal structures are presented in Table 1. In the fresh catalyst (Fig. 2 and Table 1), $Bi_2(MoO_4)_3$, Bi_2MoO_6, MoO_3, $Fe_2(MoO_4)_3$, $FeMoO_4$, $CoMoO_4$ and $NiMoO_4$ are present. From fresh catalyst to A, the crystal diffraction signal of $Bi_2(MoO_4)_3$ is substantially weakened while that of Bi_2MoO_6 is strengthened (Fig. 2). This indicates that reaction (2) happens where [O] represents lattice oxygen, as indicated by Aykan [25] for $Bi_2(MoO_4)_3$ catalyst. However, MoO_2 is not found in A, further, $Fe_2(MoO_4)_3$ also disappears

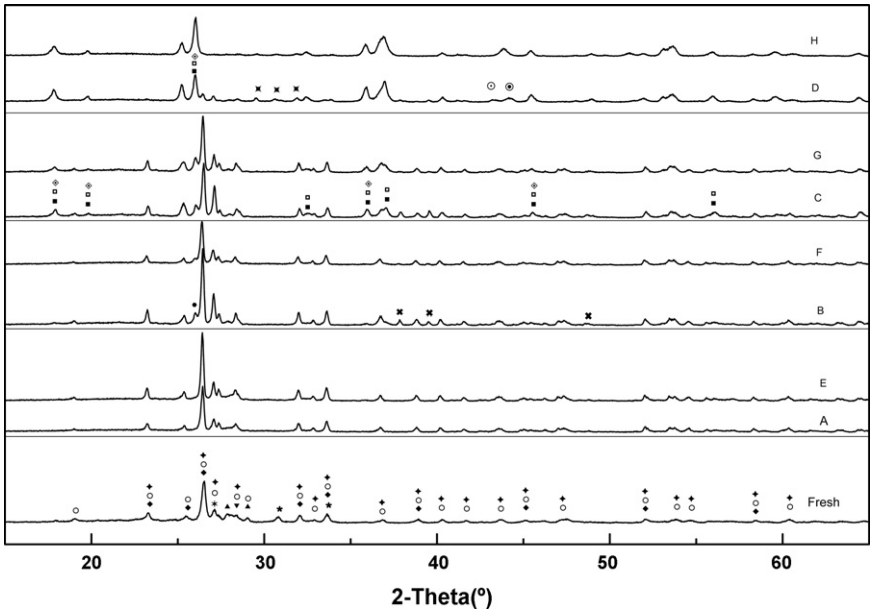

Fig. 2. XRD patterns of the fresh catalyst and the reduced catalyst: (♦) $FeMoO_4$; (○) $CoMoO_4$; (✦) $NiMoO_4$; (✱) $Fe_2(MoO_4)_3$; (▲) $Bi_2(MoO_4)_3$; (▼) Bi_2MoO_6; (✶) MoO_3; (●) MoO_2; (✖) Bi; (■) $Fe_2Mo_3O_8$; (◘) $Co_2Mo_3O_8$; (◈) $Ni_2Mo_3O_8$; (◤) Bi_3Ni; (⊙) $FeNi_3$; (◉) Fe_2C.

(Fig. 2 and Table 1), thus, reaction (3) is expected to happen.

$$Bi_2(MoO_4)_3 \rightarrow Bi_2MoO_6 + 2MoO_2 + 2[O] \quad (2)$$

$$Fe_2(MoO_4)_3 + MoO_2 \rightarrow 2FeMoO_4 + 2MoO_3 \quad (3)$$

Comparing A and B (Table 1), Bi and MoO_2 are found in B, thus reaction (4) can be expected.

$$Bi_2MoO_6 \rightarrow 2Bi + MoO_2 + 4[O] \quad (4)$$

Reactions (2)–(4) are possibly the main reason that gives rise to the loss of elements Mo and Bi in practical industrial production [33,34]. When comparing B and C (Table 1), $Fe_2Mo_3O_8$, $Co_2Mo_3O_8$ and $Ni_2Mo_3O_8$ appear in C, thus, reaction (5) happens.

$$2(Fe/Co/Ni)MoO_4 + MoO_2 \rightarrow (Fe/Co/Ni)_2Mo_3O_8 + 2[O] \quad (5)$$

For D, Table 1 indicates that it has lost activity.

The Raman spectrum for the fresh catalyst is presented in Fig. 3. As reported in literatures, the intense peak at 940 cm^{-1} is mainly attributed to characteristic band for $NiMoO_4$ [35] and $CoMoO_4$ [36], the peak at 879 cm^{-1} is mainly attributed to characteristic band for $Bi_2(MoO_4)_3$ [37] and $CoMoO_4$ [36], the peak at 820 cm^{-1} is mainly attributed to characteristic band for Bi_2MoO_6 [38] and $Fe_2(MoO_4)_3$ [39], the peak at 700 cm^{-1} is mainly attributed to characteristic band for $Bi_2(MoO_4)_3$ [37] and Bi_2MoO_6 [38]. The clear characteristic peaks for MoO_3 [40] and $FeMoO_4$ [41] are not observed, suggesting that most of MoO_3 and $FeMoO_4$ are possibly in the bulk of the fresh catalyst. The Raman spectra for the reduced catalysts are presented in Fig. 3. From fresh catalyst to A, the peaks at 879 cm^{-1} of A is weaker than that of the fresh one, suggesting that the quantity of $Bi_2(MoO_4)_3$ in A is less than that in the fresh one. According to the literature [25], $Bi_2(MoO_4)_3$ is reduced to Bi_2MoO_6. So the intensity of the peak at 820 cm^{-1} in A should be stronger than that of the fresh one. However, the peak intensity at 820 cm^{-1} in A has almost no change, suggesting that the peak intensity of $Fe_2(MoO_4)_3$ in A should be less than that of the fresh one, i.e., $Fe_2(MoO_4)_3$ is reduced. From A to B, the peak intensity at 820 cm^{-1} in B is less than that in A and the peak intensity at 700 cm^{-1} in B is very weak, suggesting the quantity of Bi_2MoO_6 declines. From B to C, the new peaks at around 675 and 570 cm^{-1} are found, which are possibly attributed to $Fe_2Mo_3O_8$, $Co_2Mo_3O_8$ and $Ni_2Mo_3O_8$, and attributed to lattice oxygen vacancies [42], respectively. From C to D, the Raman peaks change a lot. The clear characteristic peak for MoO_2 at 992 cm^{-1} is observed. The catalyst D has lost its activity. The results of LRS are in agreement with that of XRD.

Combined with the fact that the lattice oxygen of bismuth molybdate participates the propylene ammoxidation reaction

Table 1
Crystal structures of fresh, reduced and reoxidized catalysts, along with their treatment description.[a].

Catalysts	Treatment	Crystal structures
Fresh	From SRIPT, China	MoO_3, $Fe_2(MoO_4)_3$, $FeMoO_4$, $Bi_2(MoO_4)_3$, Bi_2MoO_6, $CoMoO_4$, $NiMoO_4$
A	Reduced by propylene/ammonia for 15 s at 450 °C	MoO_3, $FeMoO_4$, $Bi_2(MoO_4)_3$, Bi_2MoO_6, $CoMoO_4$, $NiMoO_4$
B	Reduced by propylene/ammonia for 30 s at 450 °C	MoO_3, $FeMoO_4$, $Bi_2(MoO_4)_3$, Bi_2MoO_6, $CoMoO_4$, $NiMoO_4$, Bi, MoO_2
C	Reduced by propylene/ammonia for 45 s at 450 °C	MoO_3, $FeMoO_4$, $Bi_2(MoO_4)_3$, Bi_2MoO_6, $CoMoO_4$, $NiMoO_4$, Bi, MoO_2, $Fe_2Mo_3O_8$, $Co_2Mo_3O_8$, $Ni_2Mo_3O_8$
D	Reduced by propylene/ammonia for 60 s at 450 °C	Bi, MoO_2, $Fe_2Mo_3O_8$, $Co_2Mo_3O_8$, $Ni_2Mo_3O_8$, $FeNi_3$, Bi_3Ni, Fe_2C
E	Reduced by hydrogen for 10 s at 450 °C	MoO_3, $FeMoO_4$, $Bi_2(MoO_4)_3$, Bi_2MoO_6, $CoMoO_4$, $NiMoO_4$
F	Reduced by hydrogen for 25 s at 450 °C	MoO_3, $FeMoO_4$, $Bi_2(MoO_4)_3$, Bi_2MoO_6, $CoMoO_4$, $NiMoO_4$, Bi, MoO_2
G	Reduced by hydrogen for 40 s at 450 °C	MoO_3, $FeMoO_4$, $Bi_2(MoO_4)_3$, Bi_2MoO_6, $CoMoO_4$, $NiMoO_4$, Bi, MoO_2, $Fe_2Mo_3O_8$, $Co_2Mo_3O_8$, $Ni_2Mo_3O_8$
H	Reduced by hydrogen for 55 s at 450 °C	Bi, MoO_2, $Fe_2Mo_3O_8$, $Co_2Mo_3O_8$, $Ni_2Mo_3O_8$, $FeNi_3$, Bi_3Ni
Reoxidized A–C; reoxidized E–G	Reoxidized by oxygen from 200 to 600 °C	MoO_3, $Fe_2(MoO_4)_3$, $FeMoO_4$, $Bi_2(MoO_4)_3$, Bi_2MoO_6, $CoMoO_4$, $NiMoO_4$

[a] Catalysts D and H are inactive, and their reoxidation are not performed.

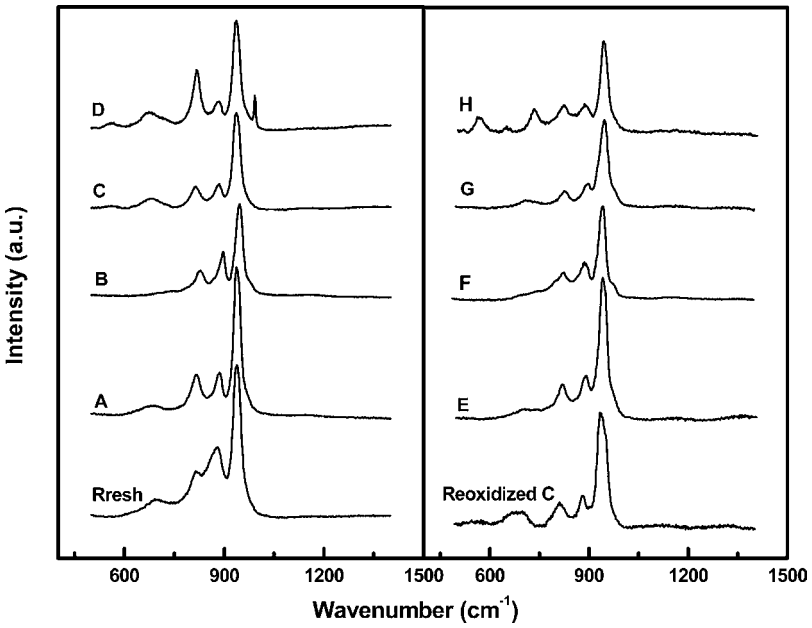

Fig. 3. Raman spectra of fresh, reduced and reoxidized catalysts.

[43,44], reactions from (2)–(5) indicate that during the propylene ammoxidation the lattice oxygen migration happens from $Fe_2(MoO_4)_3$, (Fe/Co/Ni)MoO_4 to bismuth molybdate by bulk phase diffusion. Such a lattice oxygen migration is different from the co-feed situation like Cherry-like Model [45] where lattice oxygen migration only happens between $Fe_2(MoO_4)_3$/$FeMoO_4$ and bismuth molybdate and (Co/Ni)MoO_4 as the core is only providing the host structure for Fe^{2+}. Thus, for such a multicomponent molybdate catalyst used in this work, (a) the oxygen storage capacity of catalyst is not only related to the content of bismuth molybdate, but also to the content of $Fe_2(MoO_4)_3$ and (Fe/Co/Ni)MoO_4; b) the lattice oxygen migration range is extended from iron molybdates to cobalt/nickel molybdate, and Fe^{3+}/Fe^{2+} enhances the lattice oxygen migration [26,43], thus the content of Fe is supposed to increase for the catalyst used in CFB.

In order to compare the activity of the fresh and reduced catalysts, the propylene conversion and AN selectivity for fresh catalyst reduced by propylene/ammonia with increasing reduction time are shown in Fig. 4. Both of them showed a monotonic increase with increasing reduction degree at the beginning. However, they sharp decrease after reduction time reaches 45 s. According to the above XRD and LRS results, the structures of the bulk and surface of the catalyst D have been changed when the fresh catalyst was reduced for 60 s. It indicates that a small quantity of air should be injected into riser of CFB in order to prevent the catalyst being over reduced.

3.1.2. Reduction by hydrogen

XRD patterns and the Raman spectrum of E, F, G and H are shown in Figs. 2 and 3 respectively, along with the results of catalysts A, B, C and D for comparison. As shown in Figs. 2 and 3, the crystal and surface structures of E, F and G are similar to that of A, B and C, respectively. The results indicate that the catalyst partially reduced by hydrogen has the similar lattice and surface structure as the catalyst partially reduced by mixed gas of propylene and ammonia under the similar conditions. The reoxidation process of the reduced catalyst by hydrogen is the replenishment of lattice oxygen in the catalyst, not affected by carbon deposition during propylene ammoxidation in the absence of gaseous oxygen. Therefore, the catalyst after reduced by hydrogen can be used to study reoxidation of catalyst.

3.2. Reoxidation of catalyst

The XRD results of the reoxidized catalysts are similar to that of the fresh one (Table 1). Reoxidation is therefore able to effectively restore crystal structures of the catalyst. The Raman spectra of the reoxidized catalysts are similar, taking an example for reoxidized C shown in Fig. 3. Comparing with the fresh one, no new peak is observed on the Raman spectra of reoxidized catalyst, but the intensity of these peaks is weaker, suggesting that the quantity of molybdates in the reoxidized catalyst surface is lower than that in the fresh one. The propylene conversion and AN selectivity for the fresh and reoxidized catalysts reduced by propylene/ammonia for 30 s are shown in Fig. 5. Comparing with that of the fresh, the propylene conversion and the AN selectivity for reoxidized catalysts are lower. According to the literature [34], the loss of the element Mo happens when the reoxidation temperature is close to 600 °C, resulting in low activity of the catalyst. It is likely that the activity of the reoxidized catalyst declines due to

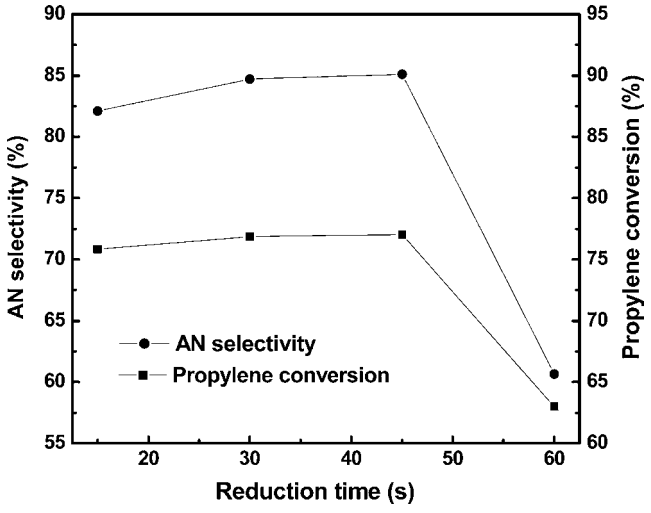

Fig. 4. Propylene conversion and AN selectivity of the fresh catalyst with increasing reduction time.

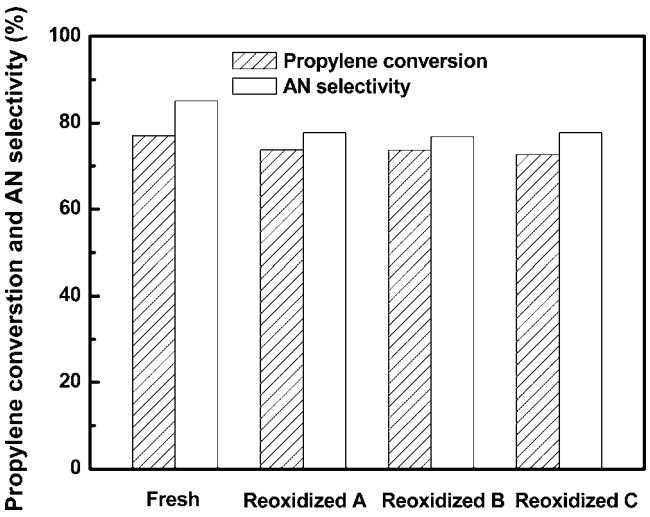

Fig. 5. Propylene conversion and AN selectivity for the fresh and reoxidized catalysts reduced by propylene/ammonia for 30 s.

over high reoxidation temperature (high to 600 °C) in this experiment.

Since the catalyst reacts with propylene/ammonia and is finally reduced to C in the absence of gaseous oxygen which is demonstrated above, the reoxidation mechanism of C in regenerator is needed. Due to that propylene ammoxidation in the absence of gaseous oxygen results into the carbon deposition on catalyst [25], the reoxidation process of C includes the replenishment of lattice oxygen and the combustion of deposited carbon. The former can is investigated through the reoxidation of the catalyst G reduced by hydrogen.

3.2.1. Replenishment of lattice oxygen

The TG/DTG curves of the reoxidation of G are shown in Fig. 6. As shown in Fig. 6, there is a mass loss from 200 to 320 °C, and this loss is ascribed to the release of adsorbed water in the interlayer of catalyst; there is a slight mass loss from 590 to 600 °C, which is probably from the sublimation of MoO_3 [45,46]; there is a mass increase from 320 to 590 °C, which is attributed to the replenishment of lattice oxygen. The sublimation of MoO_3 can explain why the quantity of the molybdates in the reoxidized catalyst surface declines. There are four peaks on DTG curve at 280 °C (peak 1), 340 °C (peak 2), 440 °C (peak 3) and 510 °C (peak 4) respectively, which indicates that there exist four reaction regions. Following the above crystal

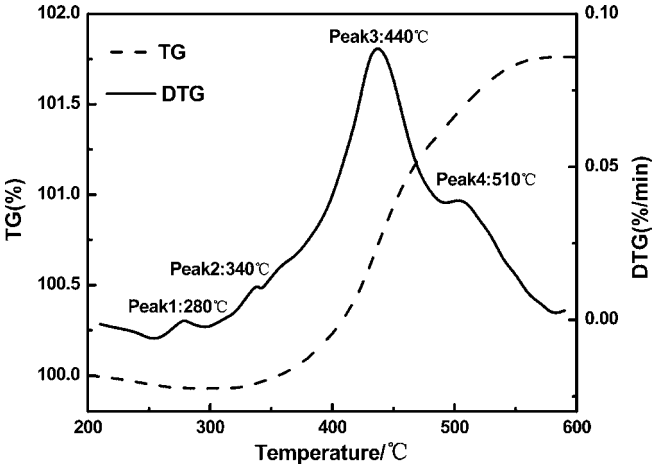

Fig. 6. TG/DTG curves of G after reoxidation.

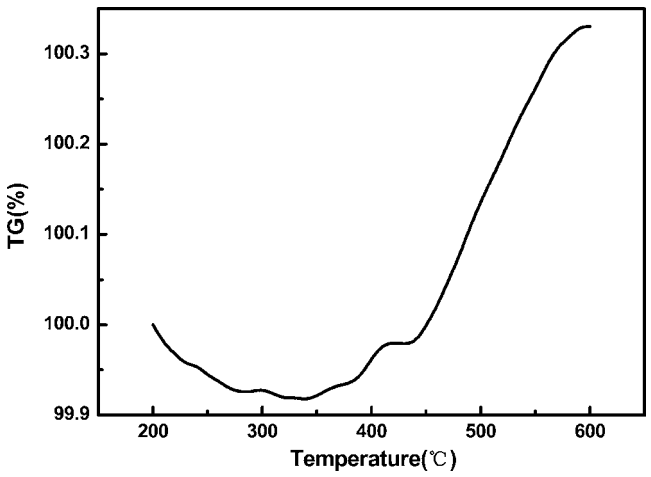

Fig. 7. TG curve of E after reoxidation.

structures (Table 1) of G, the following three reoxidation reactions can be expected

$$Fe^{2+} \xrightarrow{O_2} Fe^{3+} \quad (6)$$

$$Bi^{0} \xrightarrow{O_2} Bi^{3+} \quad (7)$$

$$Mo^{4+} \xrightarrow{O_2} Mo^{6+} \quad (8)$$

An additional reaction happens besides reaction (6)–(8).

Metal Bi can combust to Bi_2O_3 up to melt temperature of 270 °C, thus, the peak 1 at around 280 °C can be ascribed to reaction (7), i.e., the replenishment of lattice oxygen combined with Bi.

In order to further investigate the other three peaks of G, the TG curve of reoxidation of E reduced slightly is also analyzed (Fig. 7). As shown in Fig. 7, there is two regions of mass increase, i.e., 320–410 and 440–590 °C. From the XRD results of E (Fig. 2 and Table 1), the reaction (6) can be expected in reoxidation of E. Because the practical operation temperature range of propylene ammoxidation is 430–450 °C, when Fe^{2+} transforms dioxygen to lattice oxygen [26,38,43], reaction (6) should happen before 450 °C; however, mass increase does not happen from 410 to 440 °C (Fig. 7). So, the first region of mass increase from 320 to 410 °C can be ascribed to reaction (6), i.e., the replenishment of lattice oxygen that is combined with Fe. For G, peak 2 takes place between 320 and 410 °C (Fig. 6), and thus peak 2 at around 340 °C can be ascribed to the replenishment of lattice oxygen that is combined with Fe.

Comparison the TG curves of E and G, it is observed that the mass of E has no change from 410 to 440 °C, but that of G is increasing in this temperature range. So peak 3 at around 440 °C of G can be ascribed to reaction (8), i.e., the replenishment of lattice oxygen combined with Mo.

In this experiment, the former three peaks are respectively attributed to that Bi, Fe and Mo are oxidized to high valence states, apparently these are the replenishment of the bulk lattice oxygen. Thus, the peak 4 at around 510 °C of G can be ascribed to the replenishment of the additional lattice oxygen, i.e., the replenishment of the surface lattice oxygen that is the additional reaction besides reactions (6)–(8), in agreement with the results given by Brazdil [26]. While the surface lattice oxygen is responsible for deeper oxidation to CO_2/CO, and the bulk one is less active than the surface but more selective for AN [26], this implies that a lower temperature is desirable for the regeneration of catalyst. The initial temperature of the surface lattice oxygen replenishment is around 440 °C (Fig. 6). Over low temperature probably decreases the reoxidation rate of

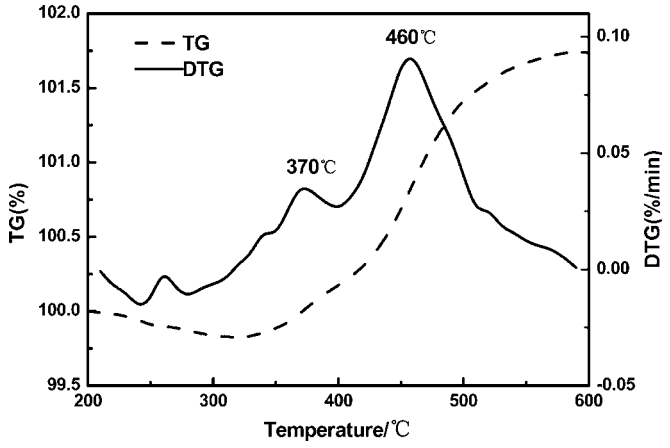

Fig. 8. TG/DTG curves of C after reoxidation.

Table 2
Comparison of reoxidation of C and G.

	C	G
Final increasing quantity of mass percent (%)	1.738	1.761
Mass loss between 200 and 320 °C (%)	0.177	0.059
Temperature of maximum mass increasing rate (°C)	460	440
Peak temperature of DTG curves (°C)	260	280
	337	340
	370	–
	460	440
	520	510

the bulk lattice oxygen (Fig. 6). Thus, it can be concluded that the favorable temperature of lattice oxygen replenishment is around 440 °C.

3.2.2. *Effect of carbon deposition*

The TG/DTG curves of C are shown in Fig. 8. Although there are the same crystal structures between C and G (Table 1), C was reduced deeper than G due to the fact that the signals of Bi and $(Fe/Co/Ni)_2Mo_3O_8$ in C were stronger than that of G (Fig. 2). Thus, after reoxidation, more mass increase from lattice oxygen replenishment was expected for C than for G. However, Table 2 indicates that the final increasing quantity of mass percent for C and G are similar; so, in the reoxidation of C, there should be additional mass loss to compensate the more increase of lattice oxygen than G, to obtain the similar increase of mass percent. The mass loss can be ascribed to the oxidation of deposited carbon on C [25], as can be indicated from the more mass loss of C than that of G between 200 and 320 °C (Table 2). Comparing the DTG curves of C and G, (a) there appears a new peak at around 370 °C on C, and this indicates that a remarkable amount of deposited carbon starts to combust tempestuously around 370 °C; (b) instead of 440 °C for G, the maximum increasing rate of mass is observed at 460 °C for C, which implies that the combustion rate of carbon before 440 °C is quicker than that after 440 °C and the combustion of deposited carbon is almost finished before 460 °C. Combined with replenishment of lattice oxygen above, the favorable reoxidation temperature is still around 440 °C.

4. Conclusions

This paper investigated reduction/reoxidation mechanism of a multicomponent molybdate catalyst for propylene ammoxidation by using XRD, LRS and thermogravimetric analysis methods. The XRD results of the catalyst with various reduced degrees demonstrate that the reduction proceeds in the order: (2)→(3)→(4)→(5), which is confirmed by the results of LRS. In the reduction process, the lattice oxygen migrates from $Fe_2(MoO_4)_3$ and $(Fe/Co/Ni)MoO_4$ to bismuth molybdate. The lattice oxygen migration range is extended, and thus the content of Fe should be properly increased in order to enhance the mobility of lattice oxygen. Thermogravimetric analysis results show that the reoxidation of the catalyst is attributed to the replenishment of the bulk lattice oxygen in the lower temperature which is respectively combined with Bi, Fe and Mo, and the replenishment of the surface lattice oxygen in the higher temperature. The favorable reoxidation temperature is around 440 °C.

Acknowledgments

This work is financially supported by the Research Fund for the Doctoral Program of Higher Education of China (20050010008), the Young Scholars Fund of Beijing University of Chemical Technology (QN0801), and National Natural Science Foundation of China (20806002).

References

[1] R.K. Grasselli, in: G. Ertel, H. Knoezinger, J. Weitkamp (Eds.), Handbook of Heterogeneous Catalysis, Wiley-VCH, 1997.
[2] R.K. Grasselli, Catal. Today 49 (1999) 141–153.
[3] P. Mars, D.W. van Krevelen, Chem. Eng. Sci. (special supp.) 3 (1954) 41–57.
[4] J.L. Callahan, R.K. Grasselli, E.C. Milberger, H.A. Strecker, I&EC (PRD) 9 (1970) 134–142.
[5] R.K. Grasselli, J.D. Burrington, Adv. Catal. 30 (1981) 133–163.
[6] Y.Q. Hu, F.Y. Zhao, F. Wei, Y. Jin, Chem. Eng. Process. 46 (2007) 918–923.
[7] G.R. Yu, X.C. Chen, H. Liu, J. Chem. Ind. Eng. 54 (2003) 1150–1154 (in Chinese).
[8] G.R. Yu, X.C. Chen, N. Xiao, J. Beijing Univ. Chem. Tech. 30 (2003) 42–47.
[9] C.Y. Li, Petrochem. Technol. Appl. 19 (2001) 272–275 (in Chinese).
[10] A. Gianetto, S. Pagliolico, G. Rovero, B. Ruggeri, Chem. Eng. Sci. 45 (1990) 2219–2225.
[11] F. Wei, F.B. Lu, Y. Jin, Z.Q. Yu, Powder Technol. 91 (1997) 189–195.
[12] F. Wei, H.F. Lin, Y. Cheng, Z.W. Wang, Y. Jin, Powder Technol. 100 (1998) 183–189.
[13] T. Nakamura, H. Arai, H. Inaba, H. Yamamoto, European Patent 0,842,922 A1 (1998).
[14] F. Wei, Y.Q. Hu, Petrochem. Technol. 27 (1998) 276–280 (in Chinese).
[15] L. Zhou, W.P. Dennler, A.R. Oroskar, B.V. Vora, H. Abrevaya, L.O. Stine, US Patent 6,143,915 (2000).
[16] F. Wei, X.T. Wan, Y.Q. Hu, Z.G. Wang, Y.H. Yang, Y. Jin, Chem. Eng. Sci. 56 (2001) 613–620.
[17] R.M. Contractor, A.W. Sleight, Catal. Today 3 (1988) 175–184.
[18] R.M. Contractor, D.I. Garnett, H.S. Horowitz, H.E. Bergna, G.S. Patience, J.T. Sihwartz, G.M. Sister, Stud. Surf. Sci. Catal. 82 (1994) 233–242.
[19] G.E. Keller, M.M. Bhasin, J. Catal. 73 (1982) 9–19.
[20] S.P. Lankhuyzen, P.M. Florack, H.S. Van der Bean, J. Catal. 42 (1976) 20–28.
[21] K.A. Shelsad, T.C. Chong, Can. J. Chem. Eng. 47 (1969) 597–602.
[22] R.K. Grasselli, J.D. Burrington, I&EC (PRD) 23 (1984) 393–404.
[23] L.K. Yong, R.F. Howe, G.W. Keulks, W.K. Hall, J. Catal. 52 (1978) 544–546.
[24] E. Ruckenstein, R. Krishnan, K.N. Rai, E. Ruckenstein, R. Krishnan, K.N. Rai, J. Catal. 45 (1976) 270–273.
[25] K. Aykan, J. Catal. 12 (1968) 281–290.
[26] J.F. Brazdil, D.D. Suresh, R.K. Grasselli, J. Catal. 66 (1980) 347–367.
[27] A.A. Firsova, Y.V. Maksimov, V.Y. Bychkov, O.V. Isaev, I.P. Suzdalev, V.N. Korchak, Kinet. Catal. 41 (2000) 116–121.
[28] S.I. Woo, J.S. Kim, H.K. Jun, J. Phys. Chem. B 108 (2004) 8941–8976.
[29] N.R. Shiju, A.J. Rondinone, D.R. Mullins, V. Schwartz, S.H. Overbury, V.V. Guliants, Chem. Mater., 2008, http://www.pubs.acs.org.
[30] M.H. Zhuang, L.N. Shen, J.X. Liu, Chem. World (special supp.) 37 (1996) 309–311 (in Chinese).
[31] J.L. Dai, J. Yu, Chem. React. Eng. Technol. 9 (1993) 345–352 (in Chinese).
[32] L.D. Krenzke, G.W. Keulks, J. Catal. 64 (1980) 295–302.
[33] L. Ma, Petrochem. Technol. 16 (1987) 292–296 (in Chinese).
[34] J.Y. Sun, Losing Activity and Regeneration of the Catalyst Chemistry, Industry Publishing, Beijing, 2006.
[35] U. Ozkan, G.L. Schrader, J. Catal. 95 (1985) 120–136.
[36] G.L. Schrader, C.P. Cheng, J. Catal. 85 (1984) 488–498.
[37] A.V. Ghule, K.A. Ghule, S.H. Tzing, J.Y. Chang, H. Chang, Y.C. Ling, Chem. Phys. Lett. 383 (2004) 208–213.
[38] I. Matsuura, R. Schut, K. Hirakawa, J. Catal. 63 (1980) 152–166.
[39] C.G. Hill, J.H. Wilson, J. Mol. Catal. A: Chem. 63 (1990) 65–94.

[40] U.S. Ozkan, M.R. Smith, S.A. Driscoll, J. Catal. 134 (1992) 24–35.
[41] N. Boucherit, A.H. Goff, S. Joiret, Corros. Sci. 32 (1991) 497–507.
[42] J.R. Mcbride, K.C. Hass, B.D. Poindexter, W.H. Weber, J. Appl. Phys. 76 (1994) 2435–2441.
[43] Y.F. Wang, J.X. Wang, C.H. Zhang, Y. Wu, Chin. J. Catal. 12 (1991) 433–438.
[44] Y. Moro-oka, W. Ueda, K.H. Lee, J. Mol. Catal. A: Chem. 199 (2003) 139–148.
[45] M.W.J. Wolfs, P.H.A. Batist, J. Catal. 32 (1974) 25–36.
[46] L.X. Zhang, D.Z. Liu, B.G. Yang, J.H. Zhao, Appl. Catal. A: Gen. 29 (1994) 163–171.